

# Discriminative Bimodal Networks for Visual Localization and Detection with Natural Language Queries

Yuting Zhang, Luyao Yuan, Yijie Guo, Zhiyuan He, I-An Huang, Honglak Lee

University of Michigan, Ann Arbor, MI, USA

{yutingzh, yuanluya, guoyijie, zhiyuan, huangian, honglak}@umich.edu

## Abstract

Associating image regions with text queries has been recently explored as a new way to bridge visual and linguistic representations. A few pioneering approaches have been proposed based on recurrent neural language models trained generatively (e.g., generating captions), but achieving somewhat limited localization accuracy. To better address natural-language-based visual entity localization, we propose a discriminative approach. We formulate a discriminative bimodal neural network (**DBNet**), which can be trained by a classifier with extensive use of negative samples. Our training objective encourages better localization on single images, incorporates text phrases in a broad range, and properly pairs image regions with text phrases into positive and negative examples. Experiments on the Visual Genome dataset demonstrate the proposed **DBNet** significantly outperforms previous state-of-the-art methods both for localization on single images and for detection on multiple images. We also establish an evaluation protocol for natural-language visual detection. Code is available at: <http://ytzhang.net/projects/dbnet>.

## 1. Introduction

Object localization and detection in computer vision are traditionally limited to a small number of predefined categories (e.g., car, dog, and person), and category-specific image region classifiers [7, 11, 14] serve as object detectors. However, in the real world, the *visual entities* of interest are much more diverse, including groups of objects (involved in certain relationships), object parts, and objects with particular attributes and/or in particular context. For scalable annotation, these entities need to be labeled in a more flexible way, such as using text phrases.

Deep learning has been demonstrated as a unified learning framework for both text and image representations. Significant progress has been made in many related tasks, such as image captioning [55, 56, 25, 37, 5, 9, 23, 18, 38], visual question answering [3, 36, 57, 41, 2], text-based fine-grained image classification [44], natural-language object retrieval [21, 38], and text-to-image generation [45].

A few pioneering works [21, 38] use recurrent neural language models [15, 39, 50] and deep image represen-

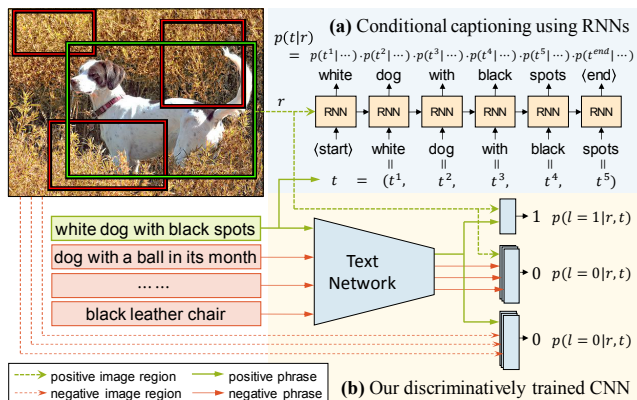


**Figure 1:** Comparison between (a) image captioning model and (b) our discriminative architecture for visual localization.

tations [31, 49] for localizing the object referred to by a text phrase given a single image (i.e., “object referring” task [26]). Global spatial context, such as “a man on the left (of the image)”, has been commonly used to pick up the particular object. In contrast, Johnson et al. [23] takes descriptions without global context<sup>1</sup> as queries for localizing more general visual entities on the Visual Genome dataset [30].

All above existing work performs localization by maximizing the likelihood to generate the query text given image regions using an image captioning model (Figure 1a), whose output probability density needs to be modeled on the virtually infinite space of the natural language. Since it is hard to train a classifier on such a huge structured output space, current captioning models are constrained to be trained in generative [21, 23] or partially discriminative [38] ways. However, as discriminative tasks, localization and detection usually favor models that are trained with a more discriminative objective to better utilize negative samples.

In this paper, we propose a new deep architecture for natural-language-based visual entity localization, which we call a *discriminative bimodal network (DBNet)*. Our architecture uses a binary output space to allow extensive discriminative training, where any negative training sample can be potentially utilized. The key idea is to take the text query as a condition rather than an output and to let the

<sup>1</sup>Only a very small portion of text phrases on the Visual Genome refer to the global context.

model directly predict if the text query and image region are compatible (Figure 1b). In particular, the two pathways of the deep architecture respectively extract the visual and linguistic representations. A discriminative pathway is built upon the two pathways to fuse the bimodal representations for binary classification of the inter-modality compatibility.

Compared to the estimated probability density in the huge space of the natural language, the score given by a binary classifier is more likely to be *calibrated*. In particular, better calibrated scores should be more comparable across different images and text queries. This property makes it possible to learn decision thresholds to determine the existence of visual entities on multiple images and text queries, making the localization model generalizable for detection tasks. While a few examples of natural-language visual detection are showcased in [23], we perform more comprehensive quantitative and ablative evaluations.

In our proposed architecture, we use convolutional neural networks (CNNs) for both visual and textual representations. Inspired by fast R-CNN [13], we use the RoI-pooling architecture induced from large-scale image classification networks for efficient feature extraction and model learning on image regions. For textual representations, we develop a character-level CNN [60] for extracting phrase features. A network on top of the image and language pathways *dynamically* forms classifiers for image region features depending on the text features, and it outputs the classifier responses on all regions of interest.

Our main contributions are as follows:

1. We develop a bimodal deep architecture with a binary output space to enable fully discriminative training for natural-language visual localization and detection.
2. We propose a training objective that extensively pairs text phrases and bounding boxes, where 1) the discriminative objective is defined over all possible region-text pairs in the entire training set, and 2) the non-mutually exclusive nature of text phrases is taken into account to avoid ambiguous training samples.
3. Experimental results on Visual Genome demonstrate that the proposed DBNet significantly outperforms existing methods based on recurrent neural language models for visual entity localization on single images.
4. We also establish evaluation methods for natural-language visual detection on multiple images and show state-of-the-art results.

## 2. Related work

**Object detection.** Recent success of deep learning on visual object recognition [31, 59, 49, 51, 53, 17] constitutes the backbone of the state-of-the-art for object detection [14, 48, 52, 61, 42, 43, 13, 46, 17, 6]. Natural-language visual detection can adapt the deep visual representations and single forward-pass computing framework (e.g., RoI pooling [13], SPP [16], R-FCN [6]) used in existing work of tra-

ditional object detection. However, natural-language visual detection needs a huge structured label space to represent the natural language, and finding a proper mapping to the huge space from visual representations is difficult.

**Image captioning and caption grounding.** The recurrent neural network (RNN) [19] based language model [15, 39, 50] has become the dominant method for captioning images with text [55]. Despite differences in details of network architectures, most RNN language models learn the likelihood of picking up a word from a predefined vocabulary given the visual appearance features and previous words (Figure 1a). Xu et al. [56] introduced an attention mechanism to encourage RNNs to focus on relevant image regions when generating particular words. Karpathy and Fei-Fei [25] used strong supervision of text-region alignment for well-grounded captioning.

**Object localization by natural language.** Recent work used the conditional likelihood of captioning an image region with given text for localizing associated objects. Hu et al. [21] proposed the spatial-context recurrent ConvNet (SCRC), which conditioned on both local visual features and global contexts for evaluating given captions. Johnson et al. [23] combined captioning and object proposal in an end-to-end neural network, which can densely caption (DenseCap) image regions and localize objects. Mao et al. [38] trained the captioning model by maximizing the posterior of localizing an object given the text phrase, which reduced the ambiguity of generated captions. However, the training objective was limited to figuring out single objects on single images. Lu et al. [34] simplified and limited text queries to subject-relationship-object (SVO) triplets. Rohrbach et al. [47] improved localization accuracy with an extra text reconstruction task. Hu et al. [20] extended bounding box localization to instance segmentation using natural language queries. Yu et al. [58] and Nagaraja et al. [40] explicitly modeled context for referral expressions.

**Text representation.** Neural networks can also embed text into a fixed-dimensional feature space. Most RNN-based methods (e.g., skip-thought vectors [29]) and CNN-based methods [24, 27] use word-level one-hot encoding as the input. Recently, character-level CNN has also been demonstrated an effective way for paragraph categorization [60] and zero-shot image classification [44].

## 3. Discriminative visual-linguistic network

The best-performing object detection framework [7, 11, 14] in terms of accuracy generally verifies if a candidate image region belongs to a particular category of interest. Though recent deep architectures [52, 46, 23] can propose regions with confidence scores at the same time, a verification model, taking as input the image features from the exact proposed regions, still serves as a key to boost the accuracy.

In this section, we develop a verification model for natural-language visual localization and detection. Unlike

the classifiers for a small number of predefined categories in traditional object detection, our model is dynamically adaptable to different text phrases.

### 3.1. Model framework

Let  $x$  be an image,  $r$  be the coordinates of a region, and  $t$  be a text phrase. The verification model  $f(x, t, r; \Theta) \in \mathbb{R}$  outputs the confidence of  $r$ 's being matched with  $t$ . Suppose that  $l \in \{1, 0\}$  is the binary label indicating if  $(t, r)$  is a positive or negative region-text pair on  $x$ . Our verification model learns to fit the probability for  $r$  and  $t$  being compatible (a positive pair), i.e.,  $p(l = 1|x, r, t)$ . See Section B in the supplementary materials for a formalized comparison with conditional captioning models.

To this end, we develop a bimodal deep neural network for our model. In particular,  $f(x, t, r; \Theta)$  is composed of two single-modality pathways followed by a discriminative pathway. The image pathway  $\phi_{\text{rgn}}(x, r; \Theta_{\text{rgn}})$  extracts the  $d_{\text{rgn}}$ -dim visual representation on the image region  $r$  on  $x$ . The language pathway  $\phi_{\text{txt}}(t; \Theta_{\text{txt}})$  extracts the  $d_{\text{txt}}$ -dim textual representation for the phrase  $t$ . The discriminative pathway with parameters  $\Theta_{\text{dis}}$  dynamically generates a classifier for visual representation according to the textual representation, and predicts if  $r$  and  $t$  are matched on  $x$ . The full model is specified by  $\Theta = (\Theta_{\text{txt}}, \Theta_{\text{rgn}}, \Theta_{\text{dis}})$ .

### 3.2. Visual and linguistic pathways

**RoI-pooling image network.** We suppose the regions of interest are given by an existing region proposal method (e.g., EdgeBox [62], RPN [46]). We calculate visual representations for all image regions in one pass using the fast R-CNN RoI-pooling pipeline. State-of-the-art image classification networks, including the 16-layer VGGNet [49] and ResNet-101 [17], are used as backbone architectures.

**Character-level textual network.** For an English text phrase  $t$ , we encode each of its characters into a 74-dim one-hot vector, where the alphabet is composed of 74 printable characters including punctuations and the space. Thus, the  $t$  is encoded as a 74-channel sequence by stacking all character encodings. We use a character-level deep CNN [60] to obtain the high-level textual representation of  $t$ . In particular, our network has 6 convolutional layers interleaving with 3 max-pooling layers and followed by 2 fully connected layers (see Section A in the supplementary materials for more details). It takes a sequence of a fixed length as the input and produces textual representations of a fixed dimension. The input length is set to be long enough (here, 256 characters) to cover possible text phrases.<sup>2</sup> To avoid empty tailing characters in the input, we replicate the text phrase until reaching the input length limit.

We empirically found that the very sparse input can easily lead to over-sparse intermediate activations, which can

<sup>2</sup>The Visual Genome dataset has more than 2.8M unique phrases, whose median length in character is 29. Less than 500 phrases has more than 100 characters.

create a large portion of ‘‘dead’’ ReLUs and finally result in a degenerate solution. To avoid this problem, we adopt the Leaky ReLU (LReLU) [35] to keep all hidden units active in the character-level CNN.

Other text embedding methods [29, 24, 27] also can be used in the DBNet framework. We use the character-level CNN because of its simplicity and flexibility. Compared to word-based models, it uses lower-dimensional input vectors and has no constraint on the word vocabulary size. Compared to RNNs, it easily allows deeper architectures.

### 3.3. Discriminative pathway

The discriminative pathway first forms a linear classifier using the textual representation of the phrase  $t$ . Its linear combination weights and bias are

$$\mathbf{w}(t) = \mathbf{A}_{\mathbf{w}}^{\top} \phi_{\text{txt}}(t; \Theta_{\text{txt}}), \quad (1)$$

$$b(t) = \mathbf{a}_{\mathbf{b}}^{\top} \phi_{\text{txt}}(t; \Theta_{\text{txt}}), \quad (2)$$

where  $\mathbf{A}_{\mathbf{w}} \in \mathbb{R}^{d_{\text{txt}} \times d_{\text{rgn}}}$ ,  $\mathbf{a}_{\mathbf{b}} \in \mathbb{R}^{d_{\text{txt}}}$ , and  $\Theta_{\text{dis}} = (\mathbf{A}_{\mathbf{w}}, \mathbf{a}_{\mathbf{b}})$ . This classifier is applied to the visual representation of the image region  $r$  on  $x$ , obtaining the verification confidence predicted by our model:

$$f(x, r, t; \Theta) = \mathbf{w}(t)^{\top} \phi_{\text{rgn}}(x, r; \Theta_{\text{rgn}}) + b(t). \quad (3)$$

Compared to the basic form of the bilinear function  $\phi_{\text{txt}}^{\top}(t; \Theta_{\text{txt}}) \mathbf{A}_{\mathbf{w}} \phi_{\text{rgn}}(x, r; \Theta_{\text{rgn}})$ , our discriminative pathway includes an additional linear term as the text-dependent bias for the visual representation classifier.

As a natural way for modeling the cross-modality correlation, multiplication is also a source of instability for training. To improve the training stability, we introduce a regularization term  $\Gamma_{\text{dynamic}} = \|\mathbf{w}(t)\|_2^2 + |b(t)|^2$  for the dynamic classifier, besides the network weight decay  $\Gamma_{\text{decay}}$  for  $\Theta$ .

## 4. Model learning

In DBNet, we drive the training of the proposed two-pathway bimodal CNN with a binary classification objective. We pair image regions and text phrases as training samples. We define the ground truth binary label for each training region-text pair (Section 4.1), and propose a weighted training loss function (Section 4.2).

**Training samples.** Given  $M$  training images  $x_1, x_2, \dots, x_M$ , let  $\mathcal{G}_i = \{(r_{ij}, t_{ij})\}_{j=1}^{N_i}$  be the set of ground truth annotations for  $x_i$ , where  $N_i$  is the number of annotations,  $r_{ij}$  is the coordinate of the  $j^{\text{th}}$  region, and  $t_{ij}$  is the text phrase corresponding to  $r_{ij}$ . When one region is paired with multiple phrases, we take each pair as a separate entry in  $\mathcal{G}_i$ .

We denote the set of all regions considered on  $x_i$  by  $\mathcal{R}_i$ , which includes both annotated regions  $\bigcup_{j=1}^{N_i} \{r_{ij}\}$  and regions given by proposal methods [54, 62, 46]. We write  $\mathcal{T}_i = \bigcup_{j=1}^{N_i} \{t_{ij}\}$  for the set of annotated text phrases on  $x_i$ , and  $\mathcal{T} = \bigcup_{i=1}^M \mathcal{T}_i$  for all training text phrases.

### 4.1. Ground truth labels

**Labeling criterion.** We assign each possible training region-text pair with a ground truth label for binary clas-

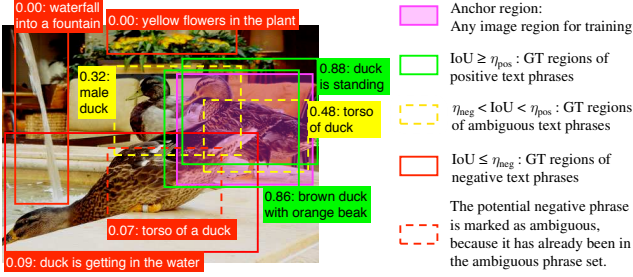


**Figure 2:** Ground truth labels for region-text pairs (given an arbitrary image region). Phrases are categorized into positive, ambiguous, and negative sets based on the given region’s overlap with ground truth boxes (measured by IoU and displayed as the numbers in front of the text phrases). Ambiguous phrases augmented by text similarity is not shown here (see the video in the supplementary materials for an illustration). For visual clarity,  $\eta_{\text{neg}} = 0.3$  and  $\eta_{\text{pos}} = 0.7$ , which are different from the rest of the paper.

sification. For a region  $r$  on the image  $x_i$  and a text phrase  $t \in \mathcal{T}_i$ , we take the largest overlap between  $r$  and  $t$ ’s ground truth regions as evidence to determine  $(r, t)$ ’s label. Let  $\text{IoU}(\cdot, \cdot)$  denote the intersection over union. The *largest overlap* is defined as

$$\nu_i(r, t) = \max_{r' \in \mathcal{R}_i} \{\text{IoU}(r', r) : (r', t) \in \mathcal{G}_i\}. \quad (4)$$

In object detection on a limited number of categories (i.e.,  $\mathcal{T}_i$  consists of category labels),  $\nu_i(r, t)$  is usually reliable enough for assigning binary training labels, given the (almost) complete ground truth annotations for all categories.

In contrast, text phrase annotations are inevitably incomplete in the training set. One image region can have an intractable number of valid textual descriptions, including different points of focus and paraphrases of the same description, so annotating all of them is infeasible. Consequently,  $\nu_i(r, t)$  cannot always reflect the consistency between an image region and a text phrase. To obtain reliable training labels, we define positive labels in a conservative manner; and then, we combine text similarity together with spatial IoU to establish the ambiguous text phrase set that reflects potential “false negative” labels. We provide detailed definitions below.

**Positive phrases.** For a region  $r$  on  $x_i$ , its positive text phrases (i.e., phrases assigned with positive labels) constitute the set

$$\mathcal{P}_i(r) = \{t \in \mathcal{T}_i : \nu_i(r, t) \geq \eta_{\text{pos}}\}, \quad (5)$$

where  $\eta_{\text{pos}}$  is a high enough IoU threshold ( $= 0.9$ ) to determine positive labels. Some positive phrases may be missing due to incomplete annotations. However, we do not try to recover them (e.g., using text similarity), as “false positive” training labels may be introduced by doing so.

**Ambiguous phrases.** Still for the region  $r$ , we collect the text phrases whose ground truth regions have moderate (neither too large nor too small) overlap with  $r$  into a set

$$\mathcal{A}_i(r) = \{t \in \mathcal{T}_i : \eta_{\text{neg}} < \nu_i(r, t) < \eta_{\text{pos}}\}, \quad (6)$$

where  $\eta_{\text{neg}}$  is the IoU lower bound ( $= 0.1$ ). When  $r$ ’s largest IoU with the ground truths of a phrase  $t$  lies in  $(\eta_{\text{neg}}, \eta_{\text{pos}})$ , it is uncertain whether  $t$  is positive or negative. In other words,  $t$  is *ambiguous* with respect to the region  $r$ .

Note that  $\mathcal{U}_i(r)$  only contains phrases from  $\mathcal{T}_i$ . To cover all possible ambiguous phrases from the full set  $\mathcal{T}$ , we use a text similarity measurement  $\text{sim}(\cdot, \cdot)$  to augment  $\mathcal{U}_i(r)$  to the finalized ambiguous phrase set

$$\mathcal{A}_i(r) = \{t \in \mathcal{T} : \exists t' \in \mathcal{U}_i(r), \text{sim}(t, t') > \tau\} \setminus \mathcal{P}_i(r), \quad (7)$$

where we use the METEOR [4] similarity for  $\text{sim}(\cdot, \cdot)$  and set the text similarity threshold  $\tau = 0.3$ .<sup>3</sup>

**Labels for region-text pairs.** For any image region  $r$  on  $x_i$  and any phrase  $t \in \mathcal{T}$ , the ground truth label of  $(r, t)$  is

$$y_i(r, t) = \begin{cases} 1, & t \in \mathcal{P}_i(r), \\ \langle \text{uncertain} \rangle, & t \in \mathcal{A}_i(r), \\ 0, & \text{otherwise,} \end{cases} \quad (8)$$

where the pairs of a region and its ambiguous text phrases are assigned with the “uncertain” label to avoid false negative labels. Figure 2 illustrates the region-text label for an arbitrary training image region.

## 4.2. Weighted training loss

**Effective training sets.** On the image  $x_i$ , the effective set of training region-text pairs is

$$\mathcal{S}_i = \{(r, t) \in \mathcal{R}_i \times \mathcal{T} : y_i(r, t) \neq \langle \text{uncertain} \rangle\}, \quad (9)$$

where, as previously defined,  $\mathcal{R}_i$  consists of annotated and proposed regions, and  $\mathcal{T}$  consists of all phrases from the training set. We exclude samples of uncertain labels.

We partition  $\mathcal{S}_i$  into three subsets according to the value of  $y_i(r, t)$  and the origin of the phrase  $t$ :  $\mathcal{S}_i^{\text{pos}}$  for  $y_i(r, t) = 1$ ,  $\mathcal{S}_i^{\text{neg}}$  for  $y_i(r, t) = 0 \wedge t \in \mathcal{T}_i$ , and  $\mathcal{S}_i^{\text{rest}}$  for all negative region-text pairs containing phrases from the rest of the training set (i.e., not from  $x_i$ ).

**Per-image training loss** Let  $f_i(r, t) = f(x_i, r, t; \Theta) \in \mathbb{R}$  for notation convenience; and, let  $\ell(\cdot, \cdot)$  be a binary classification loss, in particular, the cross-entropy loss of logistic regression. We define the training loss on  $x_i$  as the summation of three parts:

$$L_i = \lambda_{\text{pos}} L_i^{\text{pos}} + \lambda_{\text{neg}} L_i^{\text{neg}} + \lambda_{\text{rest}} L_i^{\text{rest}}, \quad (10)$$

$$L_i^{\text{pos}} = \frac{1}{|\mathcal{S}_i^{\text{pos}}|} \sum_{(r, t) \in \mathcal{S}_i^{\text{pos}}} \ell(f_i(r, t), 1), \quad (11)$$

$$L_i^{\text{neg}} = \frac{1}{|\mathcal{S}_i^{\text{neg}}|} \sum_{(r, t) \in \mathcal{S}_i^{\text{neg}}} \ell(f_i(r, t), 0), \quad (12)$$

$$L_i^{\text{rest}} = \frac{\sum_{(r, t) \in \mathcal{S}_i^{\text{rest}}} \text{freq}(t) \cdot \ell(f_i(r, t), 0)}{\sum_{(r, t) \in \mathcal{S}_i^{\text{rest}}} \text{freq}(t)}, \quad (13)$$

<sup>3</sup>If the METEOR similarity of two phrases is greater than 0.3, they are usually very similar. In Visual Genome,  $\sim 0.25\%$  of all possible pairs formed by the text phrases that occur  $\geq 20$  times can pass this threshold.

where  $\text{freq}(t)$  is  $t$ 's frequency of occurrences in the training set. We normalize and re-weight the loss for each of the three subsets of  $\mathcal{S}_i$  separately. In particular, we set  $\lambda_{\text{pos}} = \lambda_{\text{neg}} + \lambda_{\text{rest}} = 1$  to balance the positive and negative training loss. The values of  $\lambda_{\text{neg}}$  and  $\lambda_{\text{rest}}$  are implicitly determined by the numbers of text phrases that we choose inside and outside  $x_i$  during stochastic optimization.

The training loss functions in most existing work on natural-language visual localization [21, 23] use only positive samples for training, which is similar to solely using  $L_i^{\text{pos}}$ . The method in [38] also considers the negative case (similar to  $L_i^{\text{neg}}$ ), but it is less flexible and not extensible to the case of  $L_i^{\text{rest}}$ . The recurrent neural language model can encourage a certain amount of discriminativeness on word selection, but not on entire text phrases as ours.

**Full training objective.** Summing up the training loss for all images together with weight decay for the whole neural network and the regularization for the text-specific dynamic classifier (Section 3.3), the full training objective is:

$$\min_{\Theta} \frac{1}{M} \sum_{i=1}^M L_i + \beta_1 \Gamma_{\text{decay}} + \beta_2 \Gamma_{\text{dynamic}}, \quad (14)$$

where we set  $\beta_1 = 5 \times 10^{-4}$  and  $\beta_2 = 10^{-8}$ . Model optimization is in Section C of the supplementary materials.

## 5. Experiments

**Dataset.** We evaluated the proposed DBNet on the Visual Genome dataset [30]. It contains 108,077 images, where  $\sim 5\text{M}$  regions are annotated with text phrases in order to densely cover a wide range of visual entities.

We split the Visual Genome datasets in the same way as in [23]: 77,398 images for training, 5,000 for validation (tuning model parameters), and 5000 for testing; the remaining 20,679 images were not included (following [23]).

The text phrases were annotated from crowd sourcing and included a significant portion of misspelled words. We corrected misspelled words using the Enchant spell checker [1] from AbiWord. After that, there were 2,113,688 unique phrases in the training set and 180,363 unique phrases in the testing set. In the test set, about one third (61,048) of the phrases appeared in the training set, and the remaining two thirds (119,315) were unseen. About 43 unique phrases were annotated with ground truth regions per image. All experimental results are reported on this dataset.

**Models.** We constructed the fast R-CNN [13]-style visual pathway of DBNet based on either the 16-layer VGGNet (Model-D in [49]) or ResNet-101 [17]. In most experiments, we used VGGNet for fair comparison with existing works (which also use VGGNet) and less evaluation time. ResNet-101 was used to further improve the accuracy.

We compared DBNet with two image captioning based localization models: DenseCap [23] and SCRC [21]. In

DBNet, the visual pathway was pretrained for object detection using the faster R-CNN [46] on the PASCAL VOC 2007+2012 trainval set [10]. The linguistic pathway was randomly initialized. Pretrained VGGNet on ImageNet ILSVRC classification dataset [8] was used to initialize DenseCap, and the model was trained to match the dense captioning accuracy reported by Johnson et al. [23]. We found that the faster R-CNN pretraining did not benefit DenseCap (see Section E.1 of the supplementary materials). The SCRC model was additionally pretrained for image captioning on MS COCO [33] in the same way as Hu et al. [21] did.

We trained all models using the training set on Visual Genome and evaluated them for both localization on single images and detection on multiple images. We also assessed the usefulness of the major components of our DBNet.

### 5.1. Single image localization

In the localization task, we took all ground truth text phrases annotated on an image as queries to localize the associated objects by maximizing the network response over proposed image regions.

**Evaluation metrics.** We used the same region proposal method to propose bounding boxes for all models, and we used the non-maximum suppression (NMS) with the IoU threshold 0.3 to localize a few boxes. The performance was evaluated by the recall of ground truth regions of the query phrase (see Section D of the supplementary materials for a discussion on recall and precision for localization tasks). If one of the proposed bounding boxes with the top- $k$  network responses had a large enough overlap (determined by an IoU threshold) with the ground truth bounding box, we took it as a successful localization. If multiple ground truth boxes were on the same image, we only required the localized boxes to match one of them. The final recall was averaged over all test cases, i.e., per image and text phrase. Median and mean overlap (IoU) between the top-1 localized box and the ground truth were also considered.

**DBNet outperforms captioning models.** We summarize the top-1 localization performance of different methods in Table 1, where 500 bounding boxes were proposed for testing. DBNet outperforms DenseCap and SCRC under all metrics. In particular, DBNet's recall was more than twice as high as the other two methods for the IoU threshold at 0.5 (commonly used for object detection [10, 33]) and about 4 times higher for IoU at 0.7 (for high-precision localization [12, 61]).

Johnson et al. [23] reported DenseCap's localization accuracy on a much smaller test set (1000 images and 100 test queries in total), which is not comparable to our exhaustive test settings (Table 2 for comparison). We also note that different region proposal methods (EdgeBox and DenseCap RPN) did not make a big difference on the localization performance. We used EdgeBox for the rest of our evaluation.

Region proposal	Visual network	Localization model	Recall / % for IoU@							Median IoU	Mean IoU
			0.1	0.2	0.3	0.4	0.5	0.6	0.7		
DC-RPN 500	16-layer VGGNet	DenseCap	52.5	38.9	27.0	17.1	9.5	4.3	1.5	0.117	0.184
		DBNet	<b>57.4</b>	<b>46.9</b>	<b>37.8</b>	<b>29.4</b>	<b>21.3</b>	<b>13.6</b>	<b>7.0</b>	<b>0.168</b>	<b>0.250</b>
EdgeBox 500	16-layer VGGNet	DenseCap	48.8	36.2	25.7	16.9	10.1	5.4	2.4	0.092	0.178
		SCRC	52.0	39.1	27.8	18.4	11.0	5.8	2.5	0.115	0.189
		DBNet w/o bias term	52.3	43.8	36.3	29.3	22.4	15.7	9.4	0.124	0.246
		DBNet w/o VOC pretraining	54.3	45.0	36.6	28.8	21.3	14.4	8.2	0.144	0.245
		DBNet	<b>54.8</b>	<b>45.9</b>	<b>38.3</b>	<b>30.9</b>	<b>23.7</b>	<b>16.6</b>	<b>9.9</b>	<b>0.152</b>	<b>0.258</b>
	ResNet-101	DBNet	<b>59.6</b>	<b>50.5</b>	<b>42.3</b>	<b>34.3</b>	<b>26.4</b>	<b>18.6</b>	<b>11.2</b>	<b>0.205</b>	<b>0.284</b>

**Table 1:** Single-image object localization accuracy on the Visual Genome dataset. Any text phrase annotated on a test image is taken as a query for that image. “IoU@” denotes the overlapping threshold for determining the recall of ground truth boxes. DC-RPN is the region proposal network from DenseCap.

DenseCap performance	Recall / % for IoU@			Median IoU
	0.1	0.3	0.5	
Small test set in [23]	56.0	34.5	15.3	0.137
Test set in this paper	50.5	24.7	8.1	0.103

**Table 2:** Localization accuracy of DenseCap on the small test set (1000 images and 100 test queries) used in [23] and the full test set (5000 images and >0.2M queries) used in this paper. 1000 boxes (at most) per image are proposed using the DenseCap RPN.

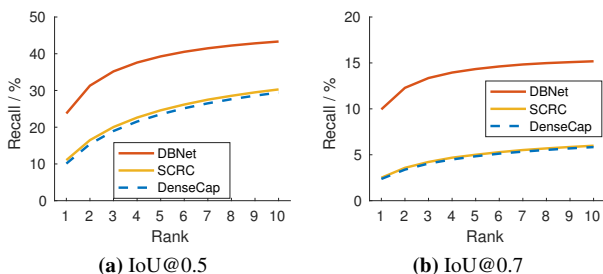


**Figure 3:** Top- $k$  localization recall under two overlapping thresholds. VGGNet and EdgeBox 500 are used in all methods.

Figure 3 shows the top- $k$  recall ( $k = 1, 2, \dots, 10$ ) in curves. SCRC is slightly better than DenseCap, possibly due to the global context features used in SCRC. DBNet outperforms both consistently with a significant margin, thanks to the effectiveness of discriminative training.

**Dynamic bias term improves performance.** The text-dependent bias term introduced in (2) and (3) makes our method for fusing visual and linguistic representations different from the basic bilinear functions (e.g., used in [44]) and more similar to a visual feature classifier. As in Table 1, this dynamic bias term led to > 20% relative improvement on median IoU and  $\sim 5\%$  (2.5%  $\sim$  0.5% absolute) relative improvement on recall at all IoU thresholds.

**Transferring knowledge benefits localization accuracy.** Pretraining the visual pathway of DBNet for object detection on PASCAL VOC showed minor benefit on recall at lower IoU thresholds, but it brought 10% and 17% relative improvement to the recall for the IoU threshold at 0.5 and 0.7, respectively. See Section E.1 in the supplementary materials for more results, where we showed that DenseCap did not get benefit from the same technique.

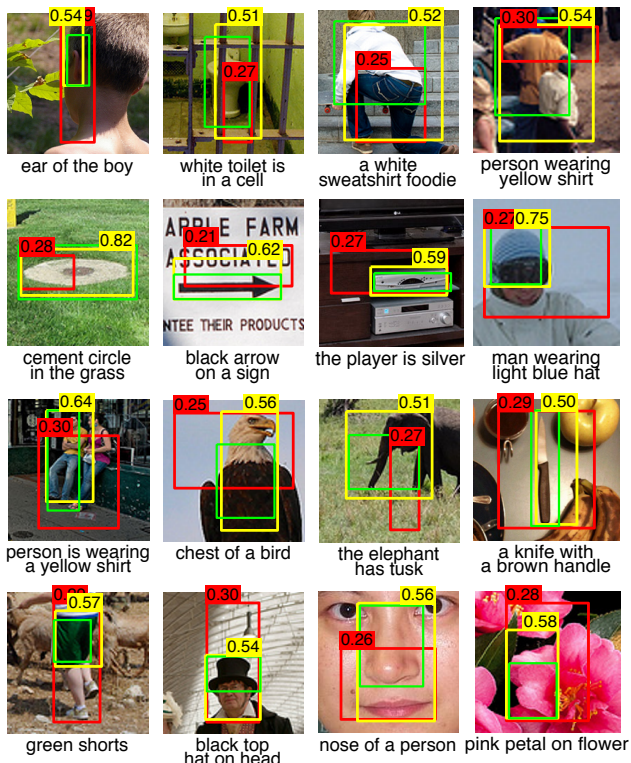


**Figure 4:** Qualitative comparison between DBNet and DenseCap on localization task. Green boxes: ground truth; Red boxes: DenseCap; Yellow boxes: DBNet.

**Qualitative results.** We visually compared the localization results of DBNet and DenseCap in Figure 4. In many cases, DBNet localized the queried entities at more reasonable locations. More examples are provided in Section F of the supplementary materials.

**More quantitative results.** In the supplementary materials, we studied the performance improvement of the learned models over random guessing and the upper bound performance due to the limitation of region proposal methods (Section E.2). We also evaluated DBNet using queries in a constrained form (Section E.3), where the high query complexity was demonstrated as a significant source of failures for natural language visual localization.

## 5.2. Detection on multiple images

In the detection task, the model needs to verify the existence and quantity of queried visual entities in addition to localizing them, if any. Text phrases not associated with any image regions can exist in the query set of an image, and evaluation metrics can be defined by extending those used in traditional object detection.

**Query sets.** Due to the huge total number of possible query phrases, it is practical to test only a subset of phrases on a test image. We developed query sets in three difficulty levels (0, 1, 2). For a text phrase, a test image is *positive* if at least one ground truth region exists for the phrase; otherwise, the image is *negative*.

- *Level-0:* The query set was the same as in the localization task, so every text phrase was tested only on its positive images (~43 phrases per image).
- *Level-1:* For each text phrase, we randomly chose the same number of negative images and the positive images (~92 phrases per image).
- *Level-2:* The number of negative images was either 5 times the number of positive images or 20 (whichever was larger) for each test phrase (~775 phrases per image). This set included relatively more negative images (compared to positive images) for infrequent phrases.

As the level went up, it became more challenging for a detector to maintain its precision, as more negative test cases are included. In the level-1 and level-2 sets, text phrases depicting obvious non-object “stuff”, such as sky, were removed to better fit the detection task. Then, 176,794 phrases (59,303 seen and 117,491 unseen) remained.

**Evaluation metrics.** We measured the detection performance by average precision (AP). In particular, we computed AP independently for each query phrase (comparable to a category in traditional object detection [10]) over its test images, and reported the *mean AP* (**mAP**) over all query phrases. Like traditional object detection, the score threshold for a detected region is category/phrase-specific.

For more practical natural-language visual detection, where the query text may not be known in advance, we also directly computed AP over all test cases. We term it *global AP* (**gAP**), which implies a universal decision threshold for any query phrase. Table 3 summarizes mAPs and gAPs under different overlapping thresholds for all models.

**DBNet shows higher per-phrase performance.** DBNet achieved consistently stronger performance than DenseCap and SCRC in terms of mAP, indicating that DBNet produced more accurate detection per given phrase. Even for the challenging IoU threshold of 0.7, DBNet still showed reasonable performance. The mAP results suggest the effectiveness of discriminative training.

**DBNet scores are better “calibrated”.** Achieving good performance in gAP is challenging as it assumes a phrase-agnostic, universal decision threshold. For IoU at 0.3 and

Average precision / %	IoU@0.3		IoU@0.5		IoU@0.7	
	mAP	gAP	mAP	gAP	mAP	gAP
DenseCap	36.2	1.8	15.7	0.5	3.4	0.0
SCRC	38.5	2.2	16.5	0.5	3.4	0.0
DBNet	<b>48.1</b>	<b>23.1</b>	<b>30.0</b>	<b>10.8</b>	<b>11.6</b>	<b>2.1</b>
DBNet w/ Res	<b>51.1</b>	<b>24.2</b>	<b>32.6</b>	<b>11.5</b>	<b>12.9</b>	<b>2.2</b>

(a) **Level-0:** Only positive images per text phrase.

Average precision / %	IoU@0.3		IoU@0.5		IoU@0.7	
	mAP	gAP	mAP	gAP	mAP	gAP
DenseCap	22.9	1.0	10.0	0.3	2.1	0.0
SCRC	37.5	1.7	16.3	0.4	3.4	0.0
DBNet	<b>45.5</b>	<b>21.0</b>	<b>28.8</b>	<b>9.9</b>	<b>11.4</b>	<b>2.0</b>
DBNet w/ Res	<b>48.3</b>	<b>22.2</b>	<b>31.2</b>	<b>10.7</b>	<b>12.6</b>	<b>2.1</b>

(b) **Level-1:** The ratio between the positive and negative images is 1:1 per text phrase.

Average precision / %	IoU@0.3		IoU@0.5		IoU@0.7	
	mAP	gAP	mAP	gAP	mAP	gAP
DenseCap	4.1	0.1	1.7	0.0	0.3	0.0
DBNet	<b>26.7</b>	<b>8.0</b>	<b>17.7</b>	<b>3.9</b>	<b>7.6</b>	<b>0.9</b>
DBNet w/ Res	<b>29.7</b>	<b>9.0</b>	<b>19.8</b>	<b>4.3</b>	<b>8.5</b>	<b>0.9</b>

(c) **Level-2:** The ratio between the positive and negative images is at least 1:5 (minimum 20 negative images and 1:5 otherwise) per text phrase.

**Table 3:** Detection average precision using query set of three levels of difficulties. mAP: mean AP over all text phrases. gAP: AP over all test cases. VGGNet is the default visual CNN for all methods. “DBNet w/ Res” denotes our DBNet with ResNet-101.

0.5, DenseCap and SCRC showed very low performance in terms of gAP, and DBNet dramatically (10 ~ 20×) outperformed them. For IoU at 0.7, DenseCap and SCRC were unsuccessful, while DBNet could produce a certain degree of positive results. The gAP results suggest that the responses of DBNet are much better calibrated among different text phrases than captioning models, supporting our hypothesis that distributions on a binary decision space are easier to model than those on the huge natural language space.

**Robustness to negative and rare cases.** The performance of all models dropped as the query set became more difficult. SCRC appeared to be more robust than DenseCap for negative test cases (level-1 performance). DBNet showed superior performance in all difficulty levels. Particularly for the level-2 query set, DenseCap’s performance dropped significantly compared to the level-1 case, which suggests that it probably failed at handling rare phrases (note that relatively more negative images are included in the level-2 set for rare phrases). For IoU at 0.5 and 0.7, DBNet’s level-2 performance was even better than the level-0 performance of DenseCap and SCRC. We did not test SCRC on the level-2 query set because of its high time consumption.<sup>4</sup>

<sup>4</sup>For level-2 query set, DBNet and DenseCap cost ~0.5 min to process one image (775 queries) when using the VGGNet and a Titan X card. SCRC takes nearly 10 minutes with the same setting. In addition, DBNet took 2–3 seconds to process one image when using level-0 query set.

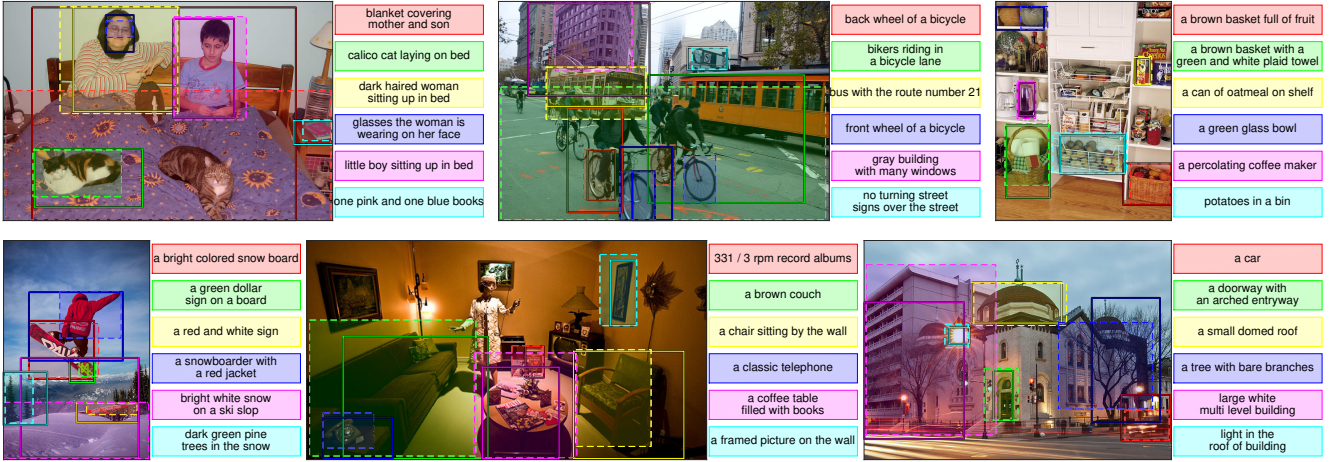


**Figure 5:** Qualitative detection results of DBNet with ResNet-101. We show detection results of six different text phrases on each image. For each image, the colors of bounding boxes correspond to the colors of text tags on the right. The semi-transparent boxes with dashed boundaries are ground truth regions, and the boxes with solid boundaries are detection results.

Prune ambiguous phrases	Phrases from other images	Finetune visual pathway	Localization					Detection (Level-1)					
			Recall / % for IoU@			Median IoU	Mean IoU	mAP / % for IoU@			gAP / % for IoU@		
			0.3	0.5	0.7			0.3	0.5	0.7	0.3	0.5	0.7
No	No	No	30.6	17.5	7.8	0.066	0.211	35.5	22.0	8.6	8.3	3.1	0.4
Yes	No	No	34.5	21.2	9.0	0.113	0.237	39.0	24.6	9.7	15.5	7.4	1.6
Yes	Yes	No	34.7	21.1	8.8	0.119	0.238	41.3	25.6	10.0	17.2	7.9	1.6
Yes	Yes	Yes	<b>38.3</b>	<b>23.7</b>	<b>9.9</b>	<b>0.152</b>	<b>0.258</b>	<b>45.5</b>	<b>28.8</b>	<b>11.4</b>	<b>21.0</b>	<b>9.9</b>	<b>2.0</b>

**Table 4:** Ablation study of DBNet’s major components. The visual pathway is based on the 16-layer VGGNet.

**Qualitative results.** We showed qualitative results of DBNet detection on selected examples in Figure 5. More comprehensive (random and failed) examples are provided in Section G of the supplementary materials. Our DBNet could detect diverse visual entities, including objects with attributes (e.g., “a bright colored snow board”), objects in context (e.g., “little boy sitting up in bed”), object parts (e.g., “front wheel of a bicycle”), and groups of objects (e.g., “bikers riding in a bicycle lane”).

### 5.3. Ablation study on training strategy

We did ablation studies for three components of our DBNet training strategy: 1) pruning ambiguous phrases ( $\mathcal{A}_i(r)$  defined in Eq. (7)), 2) training with negative phrases from other images ( $L_i^{\text{rest}}$ ), and 3) finetuning the visual pathway.

As shown in Table 4, the performance of the most basic training strategy is better than DenseCap and SCRC, due to the effectiveness of discriminative training. Ambiguous phrase pruning led to significant performance gain, by improving the correctness of training labels, where no “pruning ambiguous phrases” means setting  $\mathcal{A}_i(r) = \emptyset$ . More quantitative analysis on tuning the text similarity threshold  $\tau$  are provided in Section E.4 of the supplementary materials. Inter-image negative phrases did not benefit localization performance, since localization is a single-image task. However, this mechanism improved the detection performance by making the model more robust to diverse negative cases. As expected in most vision tasks, finetuning

pretrained classification network boosted the performance of our models. In addition, upgrading the VGGNet-based visual pathway to ResNet-101 led to another clear gain in DBNet’s performance (Table 1 and 3).

## 6. Conclusion

We demonstrated the importance of discriminative learning for natural-language visual localization. We proposed the discriminative bimodal neural network (DBNet) to allow flexible discriminative training objectives. We further developed a comprehensive training strategy to extensively and properly leverage negative observations on training data. DBNet significantly outperformed the previous state-of-the-art based on caption generation models. We also proposed quantitative measurement protocols for natural-language visual detection. DBNet showed more robustness against rare queries compared to existing methods and produced detection scores with better calibration over various text queries. Our method can be potentially improved by combining its discriminative objective with a generative objective, such as image captioning.

### Acknowledgements

This work was funded by Software R&D Center, Samsung Electronics Co., Ltd, as well as ONR N00014-13-1-0762, NSF CAREER IIS-1453651, and Sloan Research Fellowship. We thank NVIDIA for donating K40c and TITAN X GPUs. We also thank Kibok Lee, Binghao Deng, Jimei Yang, and Ruben Villegas for helpful discussions.

## References

- [1] AbiWord. Enchant spell checker. <http://www.abisource.com/projects/enchant/>. 5
- [2] J. Andreas, M. Rohrbach, T. Darrell, and D. Kleina. Neural module networks. In *CVPR*, 2016. 1
- [3] S. Antol, A. Agrawal, J. Lu, M. Mitchell, D. Batra, C. Lawrence Zitnick, and D. Parikh. VQA: Visual question answering. In *CVPR*, 2015. 1
- [4] S. Banerjee and A. Lavie. METEOR: An automatic metric for MT evaluation with improved correlation with human judgments. In *ACL workshop on intrinsic and extrinsic evaluation measures for machine translation and/or summarization*, 2005. 4
- [5] X. Chen and C. L. Zitnick. Mind’s eye: A recurrent visual representation for image caption generation. In *CVPR*, 2015. 1
- [6] J. Dai, Y. Li, K. He, and J. Sun. R-FCN: Object detection via region-based fully convolutional networks. In *NIPS*, 2016. 2
- [7] N. Dalal and B. Triggs. Histograms of oriented gradients for human detection. In *CVPR*, 2005. 1, 2
- [8] J. Deng, W. Dong, R. Socher, L.-J. Li, K. Li, and L. Fei-Fei. Imagenet: A large-scale hierarchical image database. In *CVPR*, 2009. 5, 2
- [9] J. Donahue, L. A. Hendricks, M. Rohrbach, S. Venugopalan, S. Guadarrama, K. Saenko, and T. Darrell. Long-term recurrent convolutional networks for visual recognition and description. *IEEE Transactions on Pattern Analysis and Machine Intelligence*, 39(4):677–691, April 2017. 1
- [10] M. Everingham, L. Van Gool, C. K. I. Williams, J. Winn, and A. Zisserman. The pascal visual object classes (voc) challenge. *International Journal of Computer Vision*, 88(2): 303–338, 2010. 5, 7, 2
- [11] P. Felzenszwalb, R. Girshick, D. McAllester, and D. Ramanan. Object detection with discriminatively trained part-based models. *IEEE Transactions on Pattern Analysis and Machine Intelligence*, 2010. 1, 2
- [12] A. Geiger, P. Lenz, and R. Urtasun. Are we ready for autonomous driving? the KITTI vision benchmark suite. In *CVPR*, 2012. 5
- [13] R. Girshick. Fast R-CNN. In *ICCV*, 2015. 2, 5
- [14] R. Girshick, J. Donahue, T. Darrell, and J. Malik. Region-based convolutional networks for accurate object detection and segmentation. *IEEE Transactions on Pattern Analysis and Machine Intelligence*, 38(1):142–158, Jan 2016. 1, 2
- [15] A. Graves. Generating sequences with recurrent neural networks. *arXiv:1308.0850*, 2013. 1, 2
- [16] K. He, X. Zhang, S. Ren, and J. Sun. Spatial pyramid pooling in deep convolutional networks for visual recognition. In *ECCV*, 2014. 2
- [17] K. He, X. Zhang, S. Ren, and J. Sun. Deep residual learning for image recognition. In *CVPR*, 2016. 2, 3, 5
- [18] L. A. Hendricks, S. Venugopalan, M. Rohrbach, R. Mooney, K. Saenko, and T. Darrell. Deep compositional captioning: Describing novel object categories without paired training data. In *CVPR*, 2016. 1
- [19] S. Hochreiter and J. Schmidhuber. Long short-term memory. *Neural computation*, 9(8):1735–1780, 1997. 2
- [20] R. Hu, M. Rohrbach, and T. Darrell. Segmentation from natural language expressions. In *ECCV*, 2016. 2
- [21] R. Hu, H. Xu, M. Rohrbach, J. Feng, K. Saenko, and T. Darrell. Natural language object retrieval. In *CVPR*, 2016. 1, 2, 5
- [22] Y. Jia, E. Shelhamer, J. Donahue, S. Karayev, J. Long, R. Girshick, S. Guadarrama, and T. Darrell. Caffe: Convolutional architecture for fast feature embedding. *arXiv:1408.5093*, 2014. 2
- [23] J. Johnson, A. Karpathy, and L. Fei-Fei. DenseCap: Fully convolutional localization networks for dense captioning. In *CVPR*, 2016. 1, 2, 5, 6
- [24] N. Kalchbrenner, E. Grefenstette, and P. Blunsom. A convolutional neural network for modelling sentences. In *ACL*, 2014. 2, 3
- [25] A. Karpathy and L. Fei-Fei. Deep visual-semantic alignments for generating image descriptions. In *CVPR*, 2015. 1, 2
- [26] S. Kazemzadeh, V. Ordonez, M. Matten, and T. L. Berg. Referit game: Referring to objects in photographs of natural scenes. In *EMNLP*, 2014. 1
- [27] Y. Kim. Convolutional neural networks for sentence classification. *EMNLP*, 2014. 2, 3
- [28] D. Kingma and J. Ba. Adam: A method for stochastic optimization. In *ICLR*, 2015. 2
- [29] R. Kiros, Y. Zhu, R. R. Salakhutdinov, R. Zemel, R. Urtasun, A. Torralba, and S. Fidler. Skip-thought vectors. In *NIPS*, 2015. 2, 3
- [30] R. Krishna, Y. Zhu, O. Groth, J. Johnson, K. Hata, J. Kravitz, S. Chen, Y. Kalantidis, L.-J. Li, D. A. Shamma, M. Bernstein, and L. Fei-Fei. Visual Genome: Connecting language and vision using crowdsourced dense image annotations. *International Journal of Computer Vision*, 2017. 1, 5
- [31] A. Krizhevsky, I. Sutskever, and G. E. Hinton. Imagenet classification with deep convolutional neural networks. In *NIPS*, 2012. 1, 2
- [32] Y. LeCun, B. Boser, J. S. Denker, D. Henderson, R. E. Howard, W. Hubbard, and L. D. Jackel. Backpropagation applied to handwritten zip code recognition. *Neural computation*, 1(4):541–551, 1989. 2
- [33] T.-Y. Lin, M. Maire, S. Belongie, J. Hays, P. Perona, D. Ramanan, P. Dollár, and C. L. Zitnick. Microsoft COCO: Common objects in context. In *ECCV*. 5
- [34] C. Lu, R. Krishna, M. Bernstein, and L. Fei-Fei. Visual relationship detections. In *ECCV*, 2016. 2
- [35] A. L. Maas, A. Y. Hannun, and A. Y. Ng. Rectifier nonlinearities improve neural network acoustic models. In *ICML*, 2013. 3
- [36] M. Malinowski, M. Rohrbach, and M. Fritz. Ask your neurons: A neural-based approach to answering questions about images. In *CVPR*, 2015. 1
- [37] J. Mao, W. Xu, Y. Yang, J. Wang, Z. Huang, and A. L. Yuille. Deep captioning with multimodal recurrent neural networks

- (m-RNN). In *ICLR*, 2015. 1
- [38] J. Mao, J. Huang, A. Toshev, O. Camburu, A. L. Yuille, and K. Murphy. Generation and comprehension of unambiguous object descriptions. In *CVPR*, 2016. 1, 2, 5
- [39] T. Mikolov, M. Karafiát, L. Burget, J. Cernocký, and S. Khudanpur. Recurrent neural network based language model. In *INTERSPEECH*, 2010. 1, 2
- [40] V. Nagaraja, V. Morariu, and L. Davis. Modeling context between objects for referring expression understanding. In *ECCV*, 2016. 2
- [41] H. Noh, P. H. Seo, and B. Han. Image question answering using convolutional neural network with dynamic parameter prediction. In *CVPR*, 2016. 1
- [42] W. Ouyang, X. Zeng, X. Wang, S. Qiu, P. Luo, Y. Tian, H. Li, S. Yang, Z. Wang, H. Li, C. C. Loy, K. Wang, J. Yan, and X. Tang. DeepID-Net: Deformable deep convolutional neural networks for object detection. *IEEE Transactions on Pattern Analysis and Machine Intelligence*, 2016. 2
- [43] J. Redmon, S. Divvala, R. Girshick, and A. Farhadi. You only look once: Unified, real-time object detection. In *CVPR*, 2016. 2
- [44] S. Reed, Z. Akata, B. Schiele, and H. Lee. Learning deep representations of fine-grained visual descriptions. In *IEEE Computer Vision and Pattern Recognition*, 2016. 1, 2, 6
- [45] S. Reed, Z. Akata, X. Yan, L. Logeswaran, B. Schiele, and H. Lee. Generative adversarial text-to-image synthesis. In *ICML*, 2016. 1
- [46] S. Ren, K. He, R. Girshick, and J. Sun. Faster R-CNN: Towards real-time object detection with region proposal networks. In *NIPS*, 2015. 2, 3, 5
- [47] A. Rohrbach, M. Rohrbach, R. Hu, T. Darrell, and B. Schiele. Grounding of textual phrases in images by reconstruction. In *ECCV*, 2016. 2
- [48] P. Sermanet, D. Eigen, X. Zhang, M. Mathieu, R. Fergus, and Y. LeCun. OverFeat: Integrated recognition, localization and detection using convolutional networks. In *ICLR*, 2014. 2
- [49] K. Simonyan and A. Zisserman. Very deep convolutional networks for large-scale image recognition. In *ICLR*, 2015. 1, 2, 3, 5
- [50] I. Sutskever, J. Martens, and G. E. Hinton. Generating text with recurrent neural networks. In *ICML*, 2011. 1, 2
- [51] C. Szegedy, W. Liu, Y. Jia, P. Sermanet, S. Reed, D. Anguelov, D. Erhan, V. Vanhoucke, and A. Rabinovich. Going deeper with convolutions. In *CVPR*, 2015. 2
- [52] C. Szegedy, W. Liu, Y. Jia, P. Sermanet, S. Reed, D. Anguelov, D. Erhan, V. Vanhoucke, and A. Rabinovich. Going deeper with convolutions. In *CVPR*, 2015. 2
- [53] C. Szegedy, V. Vanhoucke, S. Ioffe, J. Shlens, and Z. Wojna. Rethinking the inception architecture for computer vision. 2016. 2
- [54] J. R. Uijlings, K. E. van de Sande, T. Gevers, and A. W. Smeulders. Selective search for object recognition. *International Journal of Computer Vision*, 104(2):154–171, 2013. 3
- [55] O. Vinyals, A. Toshev, S. Bengio, and D. Erhan. Show and tell: A neural image caption generator. In *CVPR*, 2015. 1, 2
- [56] K. Xu, J. Ba, R. Kiros, K. Cho, A. Courville, R. Salakhutdinov, R. Zemel, and Y. Bengio. Show, attend and tell: Neural image caption generation with visual attention. In *ICML*, 2015. 1, 2
- [57] Z. Yang, X. He, J. Gao, L. Deng, and A. Smola. Stacked attention networks for image question answering. In *CVPR*, 2016. 1
- [58] L. Yu, P. Poirson, S. Yang, A. Berg, and T. Berg. Modeling context in referring expressions. In *ECCV*, 2016. 2
- [59] M. D. Zeiler and R. Fergus. Visualizing and understanding convolutional networks. In *ECCV*, 2014. 2
- [60] X. Zhang, J. Zhao, and Y. LeCun. Character-level convolutional networks for text classification. In *NIPS*, 2015. 2, 3
- [61] Y. Zhang, K. Sohn, R. Villegas, G. Pan, and H. Lee. Improving object detection with deep convolutional networks via bayesian optimization and structured prediction. In *CVPR*, 2015. 2, 5, 3
- [62] C. L. Zitnick and P. Dollár. Edge boxes: Locating object proposals from edges. In *ECCV*, 2014. 3, 2